



PANI: silicene nanocomposites based non-enzymatic electrochemical voltammetric sensor for dopamine detection

Gülşen Baytemir^{1,2}, Nevin Taşaltın^{2,3,4,*}, Bahriye Karaca^{2,5}, Selcan Karakuş⁶, Gamze Gürsu², Behzad Barış⁷, and Dilber Esra Yıldız^{8,*}

¹Department of Electrical and Electronics Engineering, Maltepe University, Istanbul, Turkey

²Environment and Energy Technologies Research Center, Maltepe University, Istanbul, Turkey

³Department of Basic Sciences, Maltepe University, Istanbul, Turkey

⁴CONSENS Inc, Maltepe University Research Center, Technopark Istanbul, Istanbul, Turkey

⁵Department of Industrial Engineering, Maltepe University, Istanbul, Turkey

⁶Department of Chemistry, Istanbul University-Cerrahpasa, Istanbul, Turkey

⁷Department of Physics, Giresun University, Giresun, Turkey

⁸Department of Physics, Hitit University, Corum, Turkey

Received: 23 February 2023

Accepted: 9 June 2023

Published online:

19 June 2023

© The Author(s), under exclusive licence to Springer Science+Business Media, LLC, part of Springer Nature 2023

ABSTRACT

Selective and sensitive detection of dopamine (DA) is imperative for the diagnosis and management of a wide range of neurological disorders, given its vital role as a critical neurotransmitter in the central nervous system. In this study, a series of non-enzymatic electrochemical voltammetric sensors based on polyaniline (PANI), PANI:Silicene, PANI:Coronene, and PANI:Rubrene nanocomposites (NCs) were developed for the detection of dopamine. The results showed that the PANI:Silicene NCs-based sensor exhibited a highly sensitive response towards DOP, with a sensitivity of $197.84 \mu\text{A}\mu\text{M}^{-1} \text{cm}^{-2}$ and the lowest limit of detection (LOD) of $0.0385 \mu\text{M}$. The incorporation of silicene significantly enhanced the sensor's performance in terms of both sensitivity and LOD. These findings demonstrate the potential of PANI-Silicene NC-based sensors for highly sensitive and specific detection of DOP.

1 Introduction

Dopamine (3,4-dihydroxy phenylalanine) (DOP) is a naturally produced neuromodulatory molecule in the human body that acts in the cardiovascular system, central nervous system, peripheral neural system,

and renal hormonal system [1]. As it is known, dopamine levels can be classified into three stages: 10 nM (activating normal resting/primeval effector cells), 0.1–10 μM (affecting T cells), and 0.1–1 mM (non-specific and even toxic) [2]. DOP controls various neurochemical and neurohormonal biological

Address correspondence to E-mail: nevintasaltin@maltepe.edu.tr; desrayildiz@hitit.edu.tr

functions, such as milk production, lactation, motor control, reinforcement, cognition, reward, nausea, and arousal. Therefore, the development of sensitive and selective DOP sensors is urgently needed to monitor trace levels of DOP in the diagnosis of various diseases, including COVID-19 complications, cancer, Alzheimer's, HIV infection, Parkinson's, Huntington's disease [3–7]. Consequently, the detection of DOP concentrations in blood has gained considerable attention [8–11], and the electrochemical process strategy has received considerable critical attention. Instead of expensive and difficult-to-apply methods, non-enzymatic conductive polymer-based sensors that do not require enzyme immobilization are being preferred due to their ultra-selectivity, specificity, cost-effectiveness, portability, and high reproducibility [12–14].

To improve the electrochemical performance, various materials have been investigated as electrode modifiers, including carbon dots [11], carbon quantum dots/copper oxide nanocomposite [15], Ti_3C_2 MXene [16], iron decorated multiwalled carbon nanotube (CNT) composite [17], polyaniline (PANI)/hemin/reduced graphite oxide (rGO) composite [18], poly(3,4-ethylenedioxythiophene) (PEDOT)/gold hollow nanospheres [19], polyfluorinated azobenzene/niobate composite [20], and others. Recently, PANI-based electrodes have been used in sensor applications due to their controllable electrical conductivity, environmental stability, commercial availability, and easy processability [21]. Functionalized PANI sensing systems, including ZnO decorated PAN/rGO nanocomposites [22], NiO/CuO/PANI nanocomposite [23], Ti/Ti-W-reinforced polyaniline [24], and CuO/GO/PANI nanocomposite [25], have been published in the literature for electrochemical detection of DOP. In 2020, Paulraj et al. [26] developed a novel Ag-doped PANI NCs sensor to detect hydrogen peroxide (H_2O_2) and dopamine. Electrochemical results showed that the LOD of H_2O_2 and DA were $0.03 \mu\text{M}$ and $0.12 \mu\text{M}$, respectively. In another study, Deffo et al. [13] prepared an eggshell/ CaCO_3 /PANI/rGO NC sensor to detect DOP, ascorbic acid, and uric acid. The LOD value of the sensor against DOP was $0.01 \mu\text{M}$, ascorbic acid was $10.81 \mu\text{M}$, and uric acid was $0.04 \mu\text{M}$.

Silicene exhibits excellent electrical and biological properties [27]. Additionally, coronene is a remarkable material due to its high degree of D6h symmetry-bound semi-condensed polycyclic aromatic

hydrocarbon (PAH), good load carriers, high thermostability, and strong photoluminescence properties. It consists of six benzene rings arranged in a loop molecule. Rubrene (5,6,11,12 tetraphenylnaphthalene) is a small organic semiconductor known for its charge carrier mobility, exciton emission length, and photocurrent generation efficiency [28]. It consists of phenyl (C_6H_5) tetracene (four conjoined benzene rings) base bonded to both sides of two central benzene (C_6H_6) rings and exhibits p-type semiconductor properties [29]. Furthermore, functionalized PANI sensors can facilitate fast electron transfer for detecting DOP through a redox reaction. The electrochemical performance of the prepared DOP sensors was evaluated in phosphate buffer (PBS) at pH 7.4 by simulating body fluid. Silicene, coronene, and rubrene-functionalized PANI, as well as non-functionalized PANI, showed linear responses against DOP between in concentration ranges of $0.3125\text{--}5 \mu\text{M}$. To the best of our knowledge, there are no reports on the electrochemical oxidation of DOP using prepared PANI: Silicene, PANI: Coronene and PANI: Rubrene NCs-based sensors.

2 Experimental

Coronene (molecular weight: 300.35 g/mol , 97%) and rubrene (molecular weight: 532.67 g/mol , 98%) were purchased from Sigma Aldrich Company. Silicon (Si) microparticle precursor (95%, $2 \mu\text{m}$) was purchased from Nanografi. Isopropyl alcohol (IPA) and N-Methyl-2-Pyrrolidone (NMP) (ACS, 99.8+%) were purchased from Merck Company. The gold transducers were purchased from Ebtron Electronics. Deionized water with $18.2 \text{ M}\Omega$ resistance was used. The FTIR spectra of conducting polymer blends were measured as dispersed in KBr pellets, using Varian 1000 FTIR Spectrometer. Scanning electron microscopy (SEM) (Hitachi SU 1510, Japan) is utilized for surface characterization studies. Ebtron Electronics Potentiostat was used for all electrochemical measurements. All measurements were conducted under ambient conditions ($25 \text{ }^\circ\text{C}$).

To prepare the silicene nanosheets, 100 mg of Si microparticles were sonicated in a mixture of 50 mL IPA and 50 mL deionized water at 200 W for 4 h in a nitrogen (N_2) flow-controlled cabin during the physical exfoliation process. The Si particles were then centrifuged at 5000 rpm and 12,000 rpm for

15 min, and the silicene nanosheets were collected and dried in a vacuum oven at 50 °C. To obtain the PANI: Silicene, PANI: Coronene, and PANI: Rubrene nanocomposites, 1 mg of silicene, 1 mg of coronene, and 1 mg of rubrene were separately mixed with 1 mg of polyaniline (PANI) in 2 mL of NMP solution and sonicated for 5 min. The gold transducers were cleaned using ethanol, the prepared nanoparticles were drop-casted on the gold transducers, and dried at 40 °C to obtain non-enzymatic sensors. The responses of the sensors were tested against 10 mM DOP concentration in PBS. I-V characteristics of the sensors were obtained by applying $[-1, +1]$ V with 50 mV/s scan rate at 25 °C. Then, the detection limits of the sensors were calculated using their sensitivity values.

3 Results and discussion

In this study, the morphology and lattice spacing of the silicene were investigated using selected area electron diffraction (SAED), high resolution transmission electron microscopy (HRTEM), and fast Fourier transform (FFT) techniques (Fig. 1). Few-layered free standing silicene nanosheets are shown in Fig. 1a–c. The silicene nanosheets have a highly

ordered hexagonal honeycomb lattice (Fig. 1d) and the inter-planar distance was found to be approximately $d = 0.3$ nm. Furthermore, the profile analysis shows that silicene nanosheets have a similar profile (Fig. 1e). The FFT pattern of the silicene has distinct circles of spots, each including six spots with hexagonal symmetry (Fig. 1f). All these results are the signature of silicene.

The XRD pattern of the silicene was given in Fig. 2. The analysis shows the characteristic peaks of silicene which corresponding to (111), (220), and (311) planes of centrosymmetric cubic crystal silicene with $Fd\bar{3}m$ (227) space group (JCPDS Card No. 73-1665). The unit cell parameters of the silicene are $a = 5.431$ Å, $b = 5.431$ Å, and $c = 5.431$ Å. Moreover, the rubrene

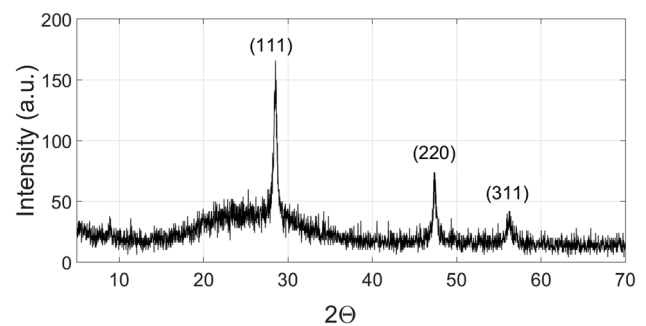
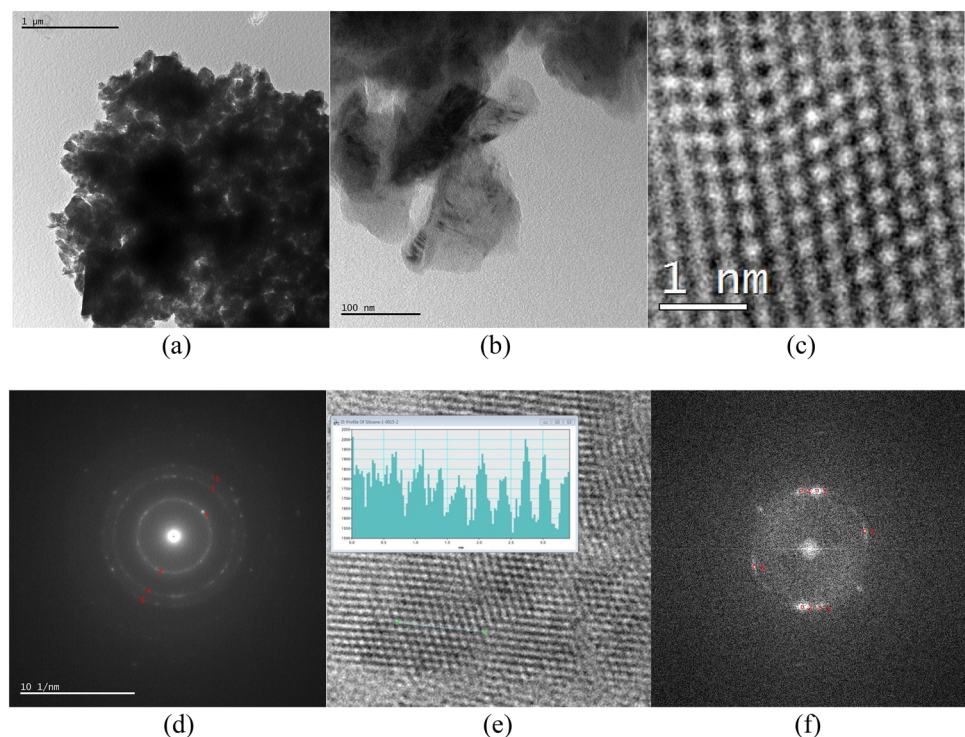


Fig. 2 XRD pattern of the silicene

Fig. 1 a–c HRTEM analysis images, d the SAED pattern, e the profile, and f the FFT pattern of the silicene



molecule has three different phases (monoclinic, orthorhombic, and triclinic). It can crystallize, but crystallizing in the orthorhombic phase is easier than the others [30, 31]. Du et al. indicated the XRD pattern of rubrene crystals for four diffraction peaks at $2\theta = 6.58, 13.08, 19.80,$ and 26.40 . The d-spacing is calculated to be $13.47 \pm 0.05 \text{ \AA}$, which is consistent with the half c-axis length of an orthorhombic unit cell (26.97 \AA) [32]. Xiao et al. indexed the coronene in space group $P2_1/n$, the unit cell parameters of the coronene are $a = 10.122 \text{ \AA}, b = 4.694 \text{ \AA}, c = 15.718 \text{ \AA},$ and $\beta = 106.02 \text{ \AA}$ [33]. The sharp diffraction peak was observed at $2\theta = 9.34$ [34].

Chemical characteristics of the PANI nanocomposites with Coronene, Silicene, and Rubrene were investigated by FTIR analysis (Fig. 3). The FTIR spectra of PANI showed peaks at 1560 cm^{-1} and 1480 cm^{-1} , attributed to the C–C stretching of the

quinonoid and benzenoid rings, respectively [35]. The FTIR spectra of PANI: Coronene showed peaks at 1590.62 cm^{-1} and 1492.73 cm^{-1} , while the FTIR spectra of PANI: Silicene showed peaks at 1590.32 cm^{-1} and 1494.10 cm^{-1} . FTIR spectra of PANI: Rubrene has peaks 1590.99 cm^{-1} and 1492.21 cm^{-1} . These peaks related to the PANI matrix in the nanocomposites shift to higher wavenumbers. These shifts may arise from π – π interaction and hydrogen bonding between PANI and coronene, silicene and rubrene. The PANI-Silicene nanocomposites showed a higher shift to higher wavenumbers than other composites, possibly due to stronger π – π interaction hydrogen bonding between Silicene and PANI. In previous works, the bands at $1295 \text{ cm}^{-1}, 1241 \text{ cm}^{-1},$ and 1125 cm^{-1} were assigned to C–H and C–N bending of quinoid rings and benzenoid for PANI [36]. These are characteristics absorption bands

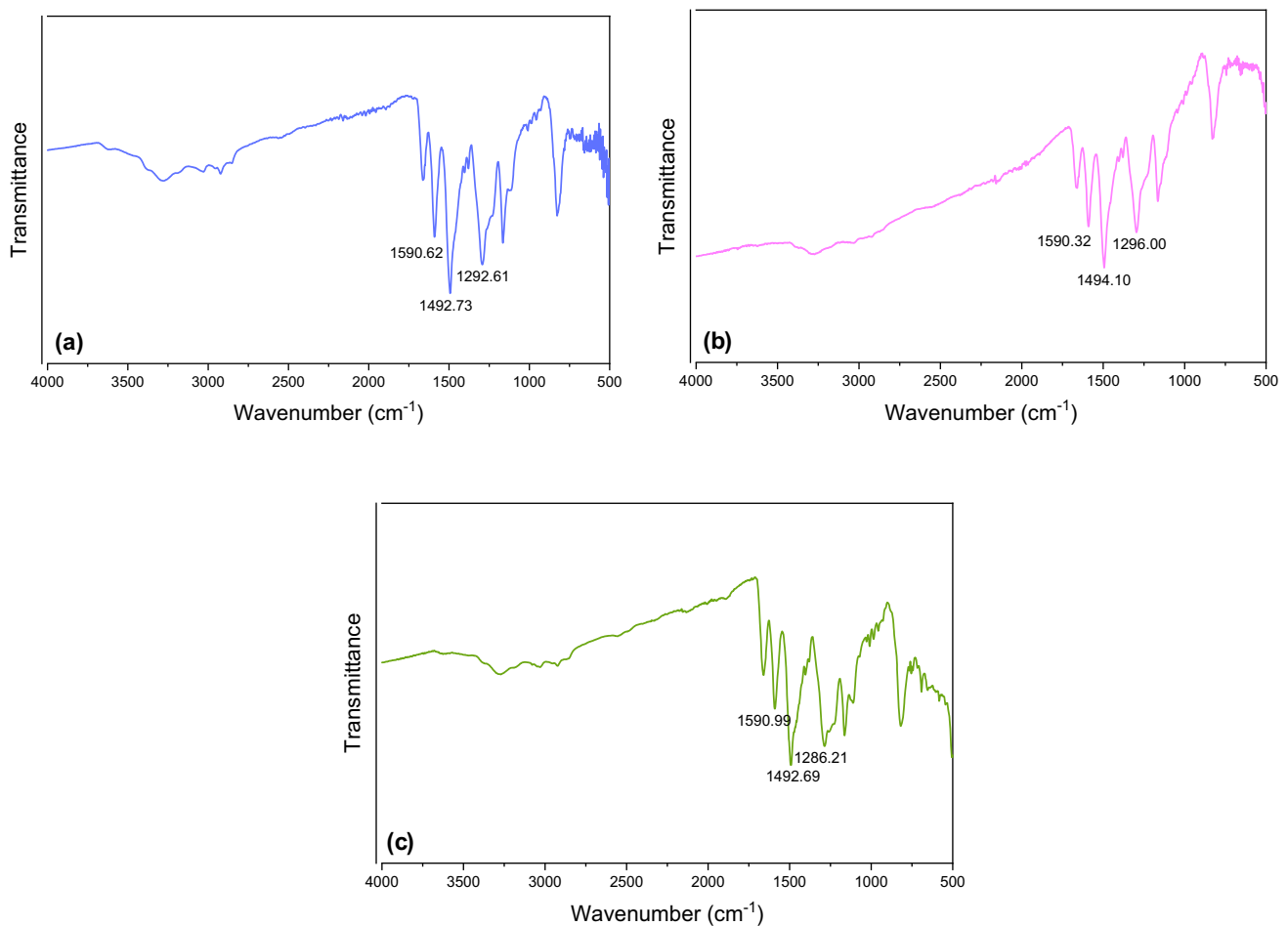


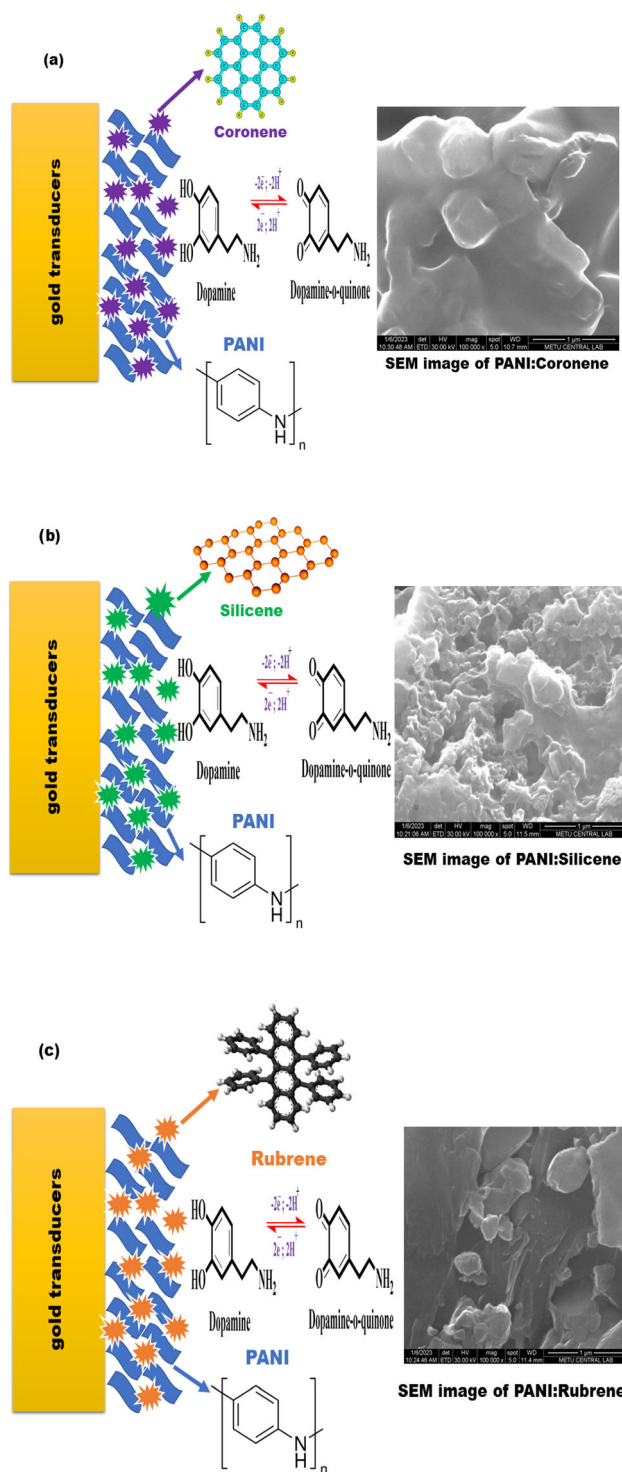
Fig. 3 FTIR spectra of **a** PANI: Coronene, **b** PANI: Silicene, and **c** PANI: Rubrene

of PANI. The FTIR spectrum of PANI: Coronene, PANI: Silicene and PANI: Rubrene showed absorption bands at 1292.61, 1296 and 1286.21 cm^{-1} , respectively. The FTIR spectra of all nanocomposites are almost the same as the FTIR spectrum of PANI [36].

A study based on obtaining a new tightly packed nanocomposite material as a result of filling conductive polymers between two-dimensional inorganic nanosheets has been carried out. Placing a conductive polymer between the nanosheets provides the advantages of providing a smooth structure to the polymer, ensuring continuity in the structure in terms of electrical conductivity, and increasing the sensor surface area. In this study, dopamine sensing characteristics of two-dimensional nanosheets coronene, rubrene and silicene were investigated comparatively. Compared to coronene and rubrene, the very easy and low cost preparation of silicene in a mixture of IPA: deionized water by physical exfoliation of silicon microparticles played a driving role in the use of silicene in this study.

The schematic representation of sensing mechanism for PANI: Coronene, PANI: Silicene and PANI: Rubrene non-enzymatic electrochemical sensor are given in Scheme 1. At this time, Scheme 1 a-c show SEM images of PANI: Coronene, PANI: Silicene and PANI: Rubrene, respectively. From the SEM image of PANI: Coronene (Scheme 1a), coronene particles are observed and the PANI: Silicene is easily agglomerated from the SEM image of the PANI: Silicene (Scheme 1b). The lamellar structures are shown from the SEM image of the PANI: Silicene (Scheme 1c).

Electrochemical measurements were carried out to detect [0.3125– 5] μM DOP for PANI, PANI: Silicene, PANI: Coronene, and PANI: Rubrene sensors (Fig. 4). All sensors have two prominent current density peaks in voltammetry measurements resulting from redox reactions of DOP with the electrode material. The results indicated that PANI: Coronene, and PANI: Rubrene sensors have similar current density peaks values. PANI: Silicene sensor, on the other hand, detected DOP with higher sensitivity due to enhanced redox mechanism resulting from silicene. The current density–voltage curves of the sensors for all concentrations are shown in Fig. 5a–d. The measured peak values of the current densities decreased with the decrease in DOP concentration for all



Scheme 1 Schematic representation of sensing mechanism a PANI: Coronene, b PANI: Silicene and c PANI: Rubrene non-enzymatic sensor with the SEM images of PANI: Coronene, PANI: Silicene and PANI: Rubrene layer

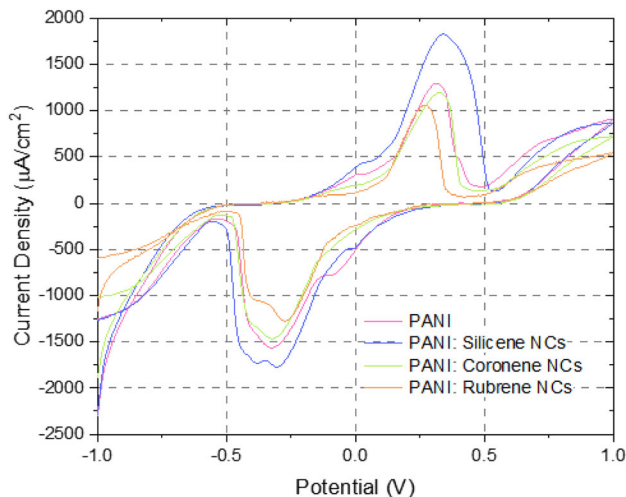


Fig. 4 Electrochemical measurement characteristics of the sensors against 5 μM DOP

sensors. The peak values of current densities versus DOP concentrations were plotted for all sensors to obtain the sensitivities from the slope of the curves (Fig. 6). The CV curves almost overlap for higher concentrations. However, there are partial deviations at higher concentrations (Figs. 4 and 5). This situation is caused by the high number of electrons coming out of the reaction due to the high concentration and these electrons creating imbalances on the sensing material while reaching the electrode surface. Another possible situation is partial deviations that may occur in the reaction mechanism at high concentrations. The sensors detected dopamine in the concentration range of 0.3125–5 μM , with the sensitivities of 134.04, 197.84, 124.65, and 133.65 $\mu\text{A}\mu\text{M}^{-1}\text{cm}^{-2}$ for PANI, PANI: Silicene, PANI: Coronene, and PANI: Rubrene sensors, respectively. Using these sensitivity values of the sensors, LOD of the PANI, PANI: Silicene, PANI: Coronene, and PANI: Rubrene sensors were calculated as 0.151 μM , 0.0385 μM , 0.122 μM , and 0.137 μM . Although the LOD values of the sensors were slightly improved by the effects of coronene and rubrene, close sensitivity values to the sensitivity of PANI-based electrode were observed. Additionally, the sensor measurements revealed that silicene considerably enhanced the sensor.

The use of modified electrodes in the electrochemical oxidation of dopamine is an effective strategy for inducing the desired redox reaction. When a

voltage is applied to the modified electrode, an electrical field is generated at the surface, causing dopamine molecules to move towards the electrode. At the electrode surface, the dopamine molecules undergo an electrochemical reaction called oxidation, which results in the loss of two electrons and two protons. This reaction converts the dopamine molecule into a highly reactive intermediate called dopamine -o-quinone molecule. During the electrochemical process, two electrons and two protons are transferred from the dopamine molecule to the electrode surface, resulting in the formation of dopamine-o-quinone. The electrochemical oxidation of dopamine on modified electrodes, such as PANI:Silicene, PANI:Coronene, and PANI:Rubrene, is a highly active area of research, and the specific mechanisms involved may vary depending on the experimental conditions. These electrodes contain PANI and aromatic hydrocarbons that function as a support and offer a large surface area for the dopamine detection. The electro-oxidation of dopamine on PANI:Silicene and PANI:Coronene involves the adsorption of dopamine on the electrode surface, followed by the transfer of electrons between the electrode and dopamine. In PANI:Silicene, the PANI component acts as a redox-active mediator, whereas in PANI:Coronene, the coronene component provides additional electron transfer pathways. Both pathways result in the oxidation of dopamine to dopamine-o-quinone molecule, which can be detected by the modified electrode [37]. PANI: Rubrene consists of rubrene, which enhances the sensitivity of DOP sensing due to its excellent electron transport properties. The electro-oxidation process on PANI: Rubrene also involves the adsorption of DOP on the electrode surface, followed by electron transfer facilitated by Rubrene. This transfer increases the sensitivity and stability of the sensor. In summary, the modified electrodes containing PANI and aromatic hydrocarbons, such as Silicene, Coronene, and Rubrene, are effective electrocatalysts for DOP sensing due to their redox-active properties and ability to facilitate electron transfer between the electrode and DOP. Consequently, the developed non-enzymatic electrochemical voltammetric sensors based on PANI, PANI:Silicene, PANI:Coronene, and PANI:Rubrene NCs have shown promising results for the detection of dopamine. Among the NCs, PANI:Silicene exhibited the highest sensitivity and lowest limit of detection, indicating its potential for highly

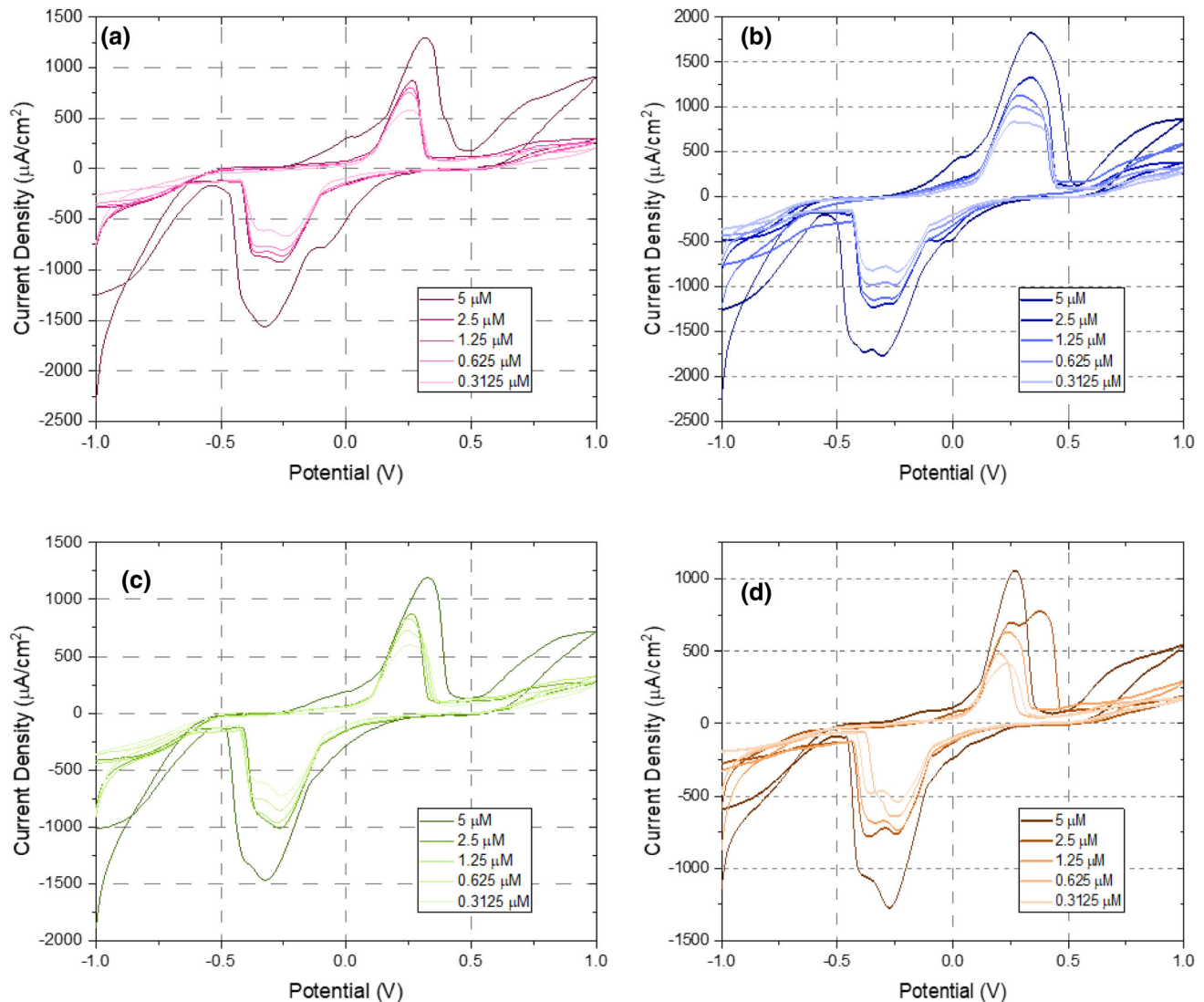


Fig. 5 Electrochemical measurement characteristics of the **a** PANI, **b** PANI: Silicene, **c** PANI: Coronene, **d** PANI: Rubrene sensors against [0.3125–5] μM DOP concentration

sensitive and specific detection of dopamine in neurological disorders.

4 Conclusion

The detection of trace levels of dopamine is essential for the diagnosis and management of various diseases, including COVID-19 complications, cancer, HIV infection, Alzheimer's, Parkinson's, and Huntington's disease. The development of sensitive and selective sensors for dopamine detection is therefore

crucial. In this study, PANI: Silicene, PANI: Coronene, and PANI: Rubrene sensors were developed for the rapid and sensitive detection of dopamine. The results showed that the PANI: Silicene sensor had the highest sensitivity of $197.84 \mu\text{A}\mu\text{M}^{-1} \text{cm}^{-2}$ and the lowest LOD of $0.0385 \mu\text{M}$. The use of silicene significantly improved the sensor's performance. These sensors could potentially be used for the early diagnosis and treatment of dopamine-related neurological disorders, thus improving patient outcomes. Further studies are needed to optimize the

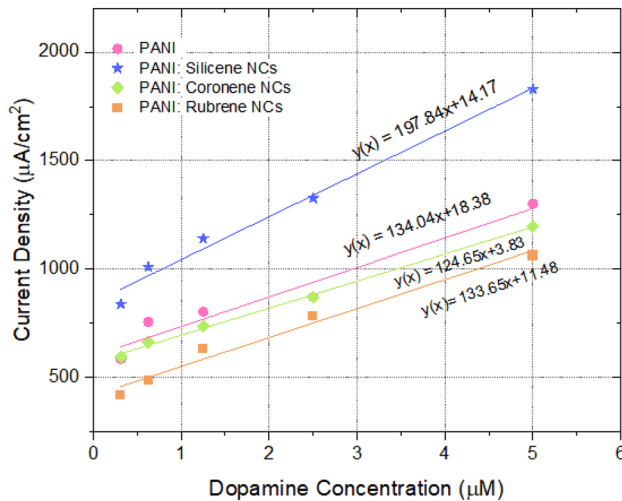


Fig. 6 The sensitivities of the sensors against DOP nanosensor design and evaluate their performance in real-life scenarios.

Acknowledgements

The authors gratefully acknowledge the Scientific and Technological Research Council of Turkey (TUBITAK) due to the financial support for the Project 122N962.

Author contributions

GB: Investigation, Methodology, Writing-original draf. NT: Investigation, Methodology, Formal analysis, Writing-original draft, Writing—review & editing, Visualization, Funding acquisition, Supervision. BK: Investigation, Methodology, Formal analysis, Writing-original draft. SK: Investigation, Methodology, Formal analysis, Writing-original draft, Writing—review & editing. GG: Investigation, Methodology, Formal analysis, Writing-original draft, Writing—review & editing. BB: Methodology, Formal analysis, Writing-original draft. DEY: Investigation, Methodology, Formal analysis, Writing-original draft, Writing—review & editing, Visualization, Funding acquisition, Supervision.

Funding

The authors have not disclosed any funding.

Data availability

The datasets generated during and/or analysed during the current study are available from the corresponding author on reasonable request.

Declarations

Conflict of interest The authors declare that they have no known competing financial interests or personal relationships that could have appeared to influence the work reported in this paper.

References

1. A. Özcan, S. İlkbaş, A. Atlılr Özcan, Development of a disposable and low-cost sensor for dopamine detection based on poly(pyrrole-3-carboxylic acid)-modified electrochemically over-oxidized pencil graphite electrode. *Talanta* **165**, 489–495 (2017)
2. Y. Feng, Y. Lu, Immunomodulatory effects of dopamine in inflammatory diseases. *Front. Immunol.* **12**, 987 (2021)
3. H.S. Han, H.K. Lee, J.M. You et al., Electrochemical biosensor for simultaneous determination of dopamine and serotonin based on electrochemically reduced GO-porphyrin. *Sens Actuators B Chem.* **190**, 886–895 (2014)
4. C. Cioates Negut, S.S. Gheorghe, R.I. Stefan-van Staden, J.F. van Staden, Fast screening test for molecular recognition of levodopa and dopamine in biological samples using 3D printed stochastic microsensors. *J. Pharm. Biomed. Anal.* **205**, 114292 (2021)
5. A. Martorana, F. di Lorenzo, Z. Esposito et al., Dopamine D2-agonist Rotigotine effects on cortical excitability and central cholinergic transmission in Alzheimer's disease patients. *Neuropharmacology* **64**, 108–113 (2013)
6. J. Luo, J.F. Collingwood, Effective R2 relaxation rate, derived from dual-contrast fast-spin echo MRI, enables detection of hemisphere differences in iron level and dopamine function in Parkinson's disease and healthy individuals. *J. Neurosci. Methods* **382**, 109708 (2022)
7. M.M. Khalefah, A.M. Khalifah, Determining the relationship between SARS-CoV-2 infection, dopamine, and COVID-19 complications. *J. Taibah Univ. Med. Sci.* **15**, 550–553 (2020)
8. A. Gottás, B.F. Ripel et al., Determination of dopamine concentrations in brain extracellular fluid using microdialysis with short sampling intervals, analyzed by ultra high performance liquid chromatography tandem mass spectrometry. *J. Pharmacol. Toxicol. Methods* **74**, 75–79 (2015)
9. M. Bouri, M.J. Lerma-García, R. Salghi et al., Selective extraction and determination of catecholamines in urine

- samples by using a dopamine magnetic molecularly imprinted polymer and capillary electrophoresis. *Talanta* **99**, 897–903 (2012)
- F. Musshoff, P. Schmidt, R. Dettmeyer et al., Determination of dopamine and dopamine derived (R)-/(S)-salsolinol and norsalsolinol in various human brain areas using solid-phase extraction and gas chromatography/mass spectrometry. *Forensic. Sci. Int.* **113**, 359–366 (2000)
 - R. Wu, S. Yu, S. Chen et al., A carbon dots-enhanced laccase-based sensor for highly sensitive detection of dopamine in human serum. *Anal. Chim. Acta* **1229**, 340365 (2022)
 - A. Üge, D. Koyuncu Zeybek, B. Zeybek, An sensor for sensitive detection of dopamine based on MWCNTs/CeO₂-PEDOT composite. *J. Electroanal. Chem.* **813**, 134–142 (2018)
 - G. Deffo, M. Basumatary, N. Hussain et al., Eggshell nano-CaCO₃ decorated PANi/rGO composite for sensitive determination of ascorbic acid, dopamine, and uric acid in human blood rum and urine. *Mater. Today Commun.* **33**, 104357 (2022)
 - F.S. Belaidi, A. Civélas, V. Castagnola et al., PEDOT-modified integrated microelectrodes for the detection of ascorbic acid, dopamine and uric acid. *Sens Actuators B Chem.* **214**, 1–9 (2015)
 - S.E. Elugoke, O.E. Fayemi, A.S. Adekunle et al., Sensor for the detection of dopamine using carbon quantum dots/copper oxide nanocomposite modified electrode. *FlatChem* **33**, 100372 (2022)
 - M. Ni, J. Chen, C. Wang et al., A high-sensitive dopamine sensor based on multilayer Ti₃C₂ MXene, graphitized multi-walled carbon nanotubes and ZnO nanospheres. *Microchem. J.* **178**, 107410 (2022)
 - H. Yang, C. Zhou, J. An et al., Ultra-fast synthesis of iron decorated multiwalled carbon nanotube composite materials: a sensitive sensor for determining dopamine. *J Alloys Compd* **897**, 163257 (2022)
 - K.P. Aryal, H.K. Jeong, Simultaneous determination of ascorbic acid, dopamine, and uric acid with polyaniline/hemin/reduced graphite oxide composite. *Chem. Phys. Lett.* **768**, 138405 (2021)
 - A. Ali, R. Jamal, T. Abdiryim, X. Huang, Synthesis of monodispersed PEDOT/Au hollow nanospheres and its application for electrochemical determination of dopamine and uric acid. *J. Electroanal. Chem.* **787**, 110–117 (2017)
 - T. Cao, Y. Zhou, H. Wang et al., Preparation of polyfluorinated azobenzene/niobate composite as sensor for detection of ascorbic acid and dopamine. *Microchem. J.* **179**, 107422 (2022)
 - T.C. Girija, M.V. Sangaranarayanan, Analysis of polyaniline-based nickel electrodes for electrochemical supercapacitors. *J Power Sources* **156**, 705–711 (2006)
 - K. Ghanbari, M. Moloudi, Flower-like ZnO decorated polyaniline/reduced graphene oxide NCs for simultaneous determination of dopamine and uric acid. *Anal. Biochem.* **512**, 91–102 (2016)
 - K. Ghanbari, Z. Babaei, Fabrication and characterization of non-enzymatic glucose sensor based on ternary NiO/CuO/polyaniline nanocomposite. *Anal Biochem* **498**, 37–46 (2016)
 - A. Krishnan, S. Beena, S.M.A. Shibli, A novel high performance Ti/Ti-W- reinforced polyaniline functionalized Ni-P electrode for high sensitive detection of dopamine from urine sample. *Mater. Chem. Phys.* **244**, 122680 (2020)
 - M. Afzali, A. Mostafavi, T. Shamspur, Square wave voltammetric determination of anticancer drug flutamide using carbon paste electrode modified by CuO/GO/PANI nanocomposite. *Arab. J. Chem.* **13**, 3255–3265 (2020)
 - P. Paulraj, A. Umar, K. Rajendran et al., Solid-state synthesis of Ag-doped PANI NCs for their end-use as an sensor for hydrogen peroxide and dopamine. *Electrochim. Acta* **363**, 137158 (2020)
 - Y. You, C. Yang, X. Zhang et al., Emerging two-dimensional silicene nanosheets for biomedical applications. *Mater. Today Nano.* **16**, 100132 (2021)
 - Fumagalli, E.M., Growth and physical properties of crystalline rubrene. 2012, Università degli Studi di Milano-Bicocca.
 - Özdemir, H.G., Spin Kaplama Yontemiyle Rubrene ince filmlerinin hazırlanması ve optik özelliklerinin incelenmesi, in Fen Bilimleri Enstitüsü. 2013, Giresun University.
 - J.-S. Kim, H. Kajii, Y. Ohmori, Characteristics of optical response in red organic light emitting diodes using two dopant system for application to the optical link devices. *Thin Solid Films* **499**(1), 343–348 (2006)
 - K.Y. Lin, Y.J. Wang, K.L. Chen, C.Y. Ho, C.C. Yang, J.L. Shen, K.C. Chiu, Role of molecular conformations in rubrene polycrystalline films growth from vacuum deposition at various substrate temperatures. *Sci. Rep.* **7**, 40824 (2017)
 - Du. Chuan, W. Wang, L. Li, H. Fuchs, L. Chi, Growth of rubrene crystalline thin films using thermal annealing on DPPC LB monolayer. *Org. Electron.* **14**, 2534–2539 (2013)
 - J. Xiao, Huiying Yang, Zongyou Yin, Jun Guo, Freddy Boey, Hua Zhang, Qichun Zhang, Preparation, characterization, and photoswitching/light-emitting behaviors of coronene nanowires. *J. Mater. Chem.* **21**, 1423–1427 (2011)
 - T.M. Krygowski, M. Cyranski, A. Ciesielski, B. Swirska, P. Leszczynski, *J. Chem. Inform. Comput. Sci.* **36**, 1135 (1996)
 - M. Shabani-Nooshabadi, F. Karimian-Taheri, Electrosynthesis of a polyaniline/zeolite nanocomposite coating on copper

- in a three-step process and the effect of current density on its corrosion protection performance. *RSC Adv.* **5**(117), 96601–96610 (2015)
36. Y. Zhang, J. Liu, Y. Zhang, J. Liu, Y. Duan, Facile synthesis of hierarchical NCs of aligned polyaniline nanorods on reduced graphene oxide nanosheets for microwave absorbing materials. *RSC Adv.* **7**, 54031–54038 (2017)
37. P. Paulraj, A. Umar, K. Rajendrane, A. Manikandana, R. Kumar, E. Manikandang, K. Pandianb, M.H. Mahnashi, M.A. Alsaiani, A.A. Ibrahimc, N. Bouropoulos, S. Baskoutas, Solid-state synthesis of Ag-doped PANI nanocomposites for their end-use as an electrochemical sensor for hydrogen peroxide and dopamine. *Electrochim. Acta* **363**, 137158 (2020)

Publisher's Note Springer Nature remains neutral with regard to jurisdictional claims in published maps and institutional affiliations.

Springer Nature or its licensor (e.g. a society or other partner) holds exclusive rights to this article under a publishing agreement with the author(s) or other rightsholder(s); author self-archiving of the accepted manuscript version of this article is solely governed by the terms of such publishing agreement and applicable law.